A comparison of surface hopping approaches for capturing metal-molecule electron transfer: A broadened classical master equation versus independent electron surface hopping

Gaohan Miao, Wenjun Ouyang, and Joseph Subotnik

Citation: J. Chem. Phys. **150**, 041711 (2019); doi: 10.1063/1.5050235
View online: https://doi.org/10.1063/1.5050235
View Table of Contents: http://aip.scitation.org/toc/jcp/150/4
Published by the American Institute of Physics

The Journal of Chemical Physics ARTICLE scitation.org/journal/jcp

A comparison of surface hopping approaches for capturing metal-molecule electron transfer: A broadened classical master equation versus independent electron surface hopping

Cite as: J. Chem. Phys. 150, 041711 (2019); doi: 10.1063/1.5050235
Submitted: 28 July 2018 • Accepted: 16 October 2018 •
Published Online: 6 December 2018

Gaohan Miao, Wenjun Ouyang, and Joseph Subotnik[a)]

AFFILIATIONS

Department of Chemistry, University of Pennsylvania, Philadelphia, Pennsylvania 19104, USA

[a)]Electronic mail: subotnik@sas.upenn.edu

ABSTRACT

Within a generalized Anderson-Holstein model, we investigate electron transfer rates using two different surface hopping algorithms: a broadened classical master equation (BCME) and independent electron surface hopping (IESH). We find that for large enough bandwidth and density of one electron states, and in the presence of external friction, the IESH results converge to the BCME results for impurity-bath model systems, recovering both relaxation rates and equilibrium populations. Without external friction, however, the BCME and IESH results can strongly disagree, and preliminary evidence suggests that IESH does not always recover the correct equilibrium state. Finally, we also demonstrate that adding an electronic thermostat to IESH does help drive the metallic substrate to the correct equilibrium state, but this improvement can sometimes come at the cost of worse short time dynamics. Overall, our results should be of use for all computational chemists looking to model either gas phase scattering or electrochemical dynamics at a metal interface.

I. INTRODUCTION

The dynamics of a molecule near a metal surface can be of a highly non-adiabatic nature,[1–7] and modeling these dynamics theoretically is still a challenge.[8–12] For a realistic calculation, a fully quantum mechanical approach is computationally prohibitive and master equation and semiclassical approaches are natural.[13–19] To that end, in recent years, several flavors of surface hopping dynamics have been proposed, including (i) independent electron surface hopping (IESH)[15] and (ii) a broadened classical master equation (BCME).[16]

Let us now review these two dynamics algorithms in more detail. First, for the last ten years, Tully's IESH generalization of the fewest switch surface hopping (FSSH) algorithm[20] has been one of the most successful algorithms for simulating gas-metal scattering dynamics.[10,21–23] The algorithm discretizes a metal bath and works effectively with a closed, but large, electronic system, and particles are propagated along adiabatic surfaces. So far, IESH has explained some features of Wodtke's NO–Au scattering experiment[1,2,9,24,25] fairly well. In particular, IESH has been able to predict accurate trapping probabilities, the rotational energies of scattered molecules, and reasonable vibrational relaxations;[21] however, it has been reported that the agreement between IESH theory and Wodtke's experiment can break down when gas molecules approach surfaces with high incidence energy,[10] and it still remains unclear exactly when IESH is reliable.

Second, let us turn to the BCME approach, which is a very new and different flavor of surface hopping which has not yet been fully tested on molecule-metal systems.[16,26,27] The algorithm is based around extrapolating a simple surface hopping master equation whereby one can model

strong molecule-metal couplings without discretizing a metal. Instead, the BCME approach approximates open system quantum dynamics in such a way that the effect of a metal surface on a nearby molecule can be incorporated with a hybridization function. The cost of the algorithm is trivial, and so far BCME has been able to predict accurate results for several model systems.[28–30] Nevertheless, the BCME approach has not been applied for a large real system; this work is ongoing in our laboratory.

With this background in mind, the goal of this article is to compare these two surface hopping algorithms (IESH vs BCME) and to assess their relative strengths and weaknesses. Of course, it can be difficult to assess semiclassical *Ansätze* without fully quantum, exact benchmark calculations, and so the primary test of the methods here will be to see if IESH recovers the Marcus theory of electron transfer (ET) in the high temperature limit; BCME has already been validated for the Marcus problem.[28] We will also investigate whether IESH recovers the correct equilibrium state. To our knowledge, no one has yet thoroughly compared IESH dynamics against Marcus theory for an Anderson-Holstein (AH) model.[6,31–34]

This paper is organized as follows: In Sec. II, we briefly discuss the AH model, before reviewing both BCME and IESH dynamics. In Sec. III, we offer simulation details and show numerical results, comparing the surface hopping algorithms. In Sec. IV, we discuss further improvements possible for the surface hopping methods. We conclude in Sec. V.

A. Notations

The notation used in this paper is as follows. We use x and p to denote the coordinate and momentum, respectively, for a single nuclear degree of freedom. Electron orbitals are denoted by normal characters (e.g., ψ), while many-electron states are denoted by bold characters (e.g., $\mathbf{\Psi}$).

II. BACKGROUND: HAMILTONIAN AND METHODS

A. Generalized Anderson-Holstein (AH) model

Consider an impurity site (with creation and annihilation operators d, $d^\dagger$) near a bath (with creation and annihilation operators c_k, $c_k^\dagger$). For such a problem, a generalized AH model is defined by the following Hamiltonian:

$$H = \frac{p^2}{2m} + U_0(x) + h(x)d^\dagger d + \int_{-W}^{W} \epsilon_k c_k^\dagger c_k dk + \int_{-W}^{W} V_k(x)(c_k^\dagger d + d^\dagger c_k)dk. \quad (1)$$

Here, x denotes a nuclear degree of freedom that modulates the energy of the impurity site. We define $U_0(x)$ and $U_1(x)$ as the potential energy surfaces (PES) when the molecule is neutral or negative charged, respectively, and $h(x)$ is defined as $U_1(x) - U_0(x)$. The bandwidth is 2W. $V_k(x)$ denotes the coupling between the impurity site and the bath orbitals labeled by k. The Fermi level of the bath is assumed to be zero throughout this paper.

In practice, for the calculations below, we discretize the bath into M orbitals, and the Hamiltonian becomes

$$H = \frac{p^2}{2m} + U_0(x) + h(x)d^\dagger d + \sum_{n=1}^{M} \epsilon_n c_n^\dagger c_n + \sum_{n=1}^{M} V_n(x)(d^\dagger c_n + c_n^\dagger d). \quad (2)$$

The discretized orbitals are labeled by n = 1, 2, . . ., M. Very often, it is helpful to consider the hybridization function $\Gamma(x, E)$ that enters into the Fermi golden rule, where $\Gamma(x, E) \equiv 2\pi \sum_{n=1}^{M} V_n^2(x)\delta(E-\epsilon_n)$. Here and below, we will apply the wide band approximation (WBA) and Condon approximation so that we assume Γ is a constant everywhere and independent of energy.

B. Classical master equation (CME)

To derive the BCME, it is helpful to first consider the classical master equation (CME) algorithm, which arises from perturbation theory in the molecule-metal coupling. For these dynamics, a trajectory is propagated with a fixed charge along a diabatic surface [either $U_0(x)$ or $U_1(x)$]. At each time step, there is a finite probability to hop to another surface, i.e., change charge state. The classical master equations can be expressed as follows:[26]

$$\begin{aligned} \partial_t P_0(x,p,t) &= -\frac{p}{m}\partial_x P_0(x,p,t) + \partial_x U_0(x)\partial_p P_0(x,p,t) \\ &\quad - \frac{\Gamma}{\hbar} f(h(x))P_0(x,p,t) + \frac{\Gamma}{\hbar}(1-f(h(x)))P_1(x,p,t), \\ \partial_t P_1(x,p,t) &= -\frac{p}{m}\partial_x P_1(x,p,t) + \partial_x U_1(x)\partial_p P_1(x,p,t) \\ &\quad + \frac{\Gamma}{\hbar} f(h(x))P_0(x,p,t) - \frac{\Gamma}{\hbar}(1-f(h(x)))P_1(x,p,t). \end{aligned} \quad (3)$$

Here $P_0(x, p, t)$ and $P_1(x, p, t)$ are probability densities for the related nuclear degree of freedom to be located at phase point (x, p) at time t in electronic states $|0\rangle$ and $|1\rangle$, respectively. $f(x)$ is the Fermi function. The CME [Eq. (3)] is derived by (i) invoking perturbation theory whereby $kT \gg \Gamma$ and (ii) assuming the classical limit $kT/\hbar \gg \sqrt{\partial_x^2 U_0(x)/m}$.

C. Electronic friction (EF): Unbroadened and broadened flavors

The polar opposite of CME dynamics is the model of electronic friction.[13,14,35–40] Electronic friction dynamics wrap up all non-adiabatic effects into a friction term and trajectories are propagated subject to this electronic friction (as well as any additional external nuclear friction). Although EF dynamics are distinctly not a flavor of surface hopping, they are important because they should be valid when surface hopping becomes invalid (i.e., the limit of large Γ).

To derive an unbroadened flavor of EF dynamics in the limit that Γ is not too large, we consider Eq. (3) and define two new probability densities

$$\begin{aligned} P_A(x,p,t) &\equiv P_0(x,p,t) + P_1(x,p,t), \\ P_B(x,p,t) &\equiv f(h(x))P_0(x,p,t) - (1-f(h(x)))P_1(x,p,t). \end{aligned} \tag{4}$$

For large enough Γ, the population on the two diabats will reach local equilibrium quickly such that $P_B(x,p,t)$ will be small and change slowly. For this case, a Fokker Plank (FP) equation for $P_A(x,p,t)$ can be derived,[26]

$$\begin{aligned} \partial_t P_A(x,p,t) = &-\frac{P}{m}\partial_x P_A(x,p,t) + \partial_x U_{unb}^{adiab}(x)\partial_p P_A(x,p,t) \\ &+ \frac{\gamma_e}{m}\partial_p(pP_A(x,p,t)) + \gamma_e kT\partial_t^2 P_A(x,p,t). \end{aligned} \tag{5}$$

When calculating $P_A(x,p,t)$ with trajectories, particles are propagated along an "adiabatic" surface,

$$\begin{aligned} U_{unb}^{adiab}(x) &= U_0(x) + \int^x f(h(x'))\partial_{x'}h(x')dx' \\ &= U_0(x) + kTln\left(1+e^{-h(x)/kT}\right), \end{aligned} \tag{6}$$

and the electronic friction is

$$\gamma_e = -\frac{\hbar}{\Gamma}(\partial_x h(x))^2\,\partial_E f(E)|_{E=h(x)}. \tag{7}$$

Now, Eqs. (5)–(7) are not the most general electronic friction model; after all, this equation was derived after first assuming small Γ and then assuming large Γ! Thus this equation cannot describe the case of very large Γ, where an impurity can hybridize with a metal surface, a phenomenon sometimes referred to as "broadening." In such a case, if $h(x)$ is the impurity's energy, the correct population is not just $f(h(x))$, but rather a broadened population that incorporates hybridization. The correctly broadened "adiabatic" surface can be found by performing a projection akin to Eq. (3), but starting with the quantum-classical Liouville equation (QCLE)[36,41–45] instead of the CME. The result is[27,46]

$$U_b^{adiab}(x) = U_0(x) + \int^x n(h(x'))\partial_{x'}h(x')dx', \tag{8}$$

where the local population on the impurity is

$$n(h(x)) \equiv \int \frac{dE}{2\pi}A(E,h(x))f(E). \tag{9}$$

Here $A(E,h(x))$ is the spectral function

$$A(E,h(x)) \equiv \frac{\Gamma}{(E-h(x))^2 + (\Gamma/2)^2}. \tag{10}$$

Furthermore, according to the QCLE (and many other approaches[35,39,40,47,48]), the correct electronic friction term is not given by Eq. (7), but rather also involves the spectral function (such that broadening is again included)

$$\gamma_{e,b} = -\frac{\hbar}{2}\int \frac{dE}{2\pi}(\partial_x h(x))^2 A^2(E,h(x))\partial_E f(E). \tag{11}$$

Equation (11) reduces to Eq. (7) in the limit that $\Gamma \to 0$.

D. Broadened classical master equation (BCME)

We may now briefly review BCME dynamics. The BCME is an extension of the CME to cases with large molecule-metal coupling, where we can no longer assume $kT \gg \Gamma$.

To incorporate broadening effects, we artificially manipulate the diabatic surfaces $U_0(x)$ and $U_1(x)$ such that trajectories are effectively propagated along the broadened adiabats U_b^{adiab} in Eq. (8). In order to achieve this replacement, a straightforward scheme is to modify the diabatic surfaces,[16,27]

$$\begin{aligned} U_0^b &= U_0 - \int_{-\infty}^x \Delta F^{BCME}(x')dx', \\ U_1^b &= U_1 - \int_{-\infty}^x \Delta F^{BCME}(x')dx', \\ \Delta F^{BCME}(x) &= -\partial_x h(x)[n(h(x)) - f(h(x))]. \end{aligned} \tag{12}$$

As a result, the BCME dynamics are defined as follows:

$$\begin{aligned} \partial_t P_0(x,p,t) = &-\frac{p}{m}\partial_x P_0(x,p,t) + \left(\partial_x U_0(x) - \Delta F^{BCME}(x)\right)\partial_p P_0(x,p,t) \\ &- \frac{\Gamma}{\hbar}f(h(x))P_0(x,p,t) + \frac{\Gamma}{\hbar}(1-f(h(x)))P_1(x,p,t), \\ \partial_t P_1(x,p,t) = &-\frac{p}{m}\partial_x P_1(x,p,t) + \left(\partial_x U_1(x) - \Delta F^{BCME}(x)\right)\partial_p P_1(x,p,t) \\ &+ \frac{\Gamma}{\hbar}f(h(x))P_0(x,p,t) - \frac{\Gamma}{\hbar}(1-f(h(x)))P_1(x,p,t). \end{aligned} \tag{13}$$

Now, note that if we consider Eq. (13) and project out the total population [as in Eq. (3)], we will necessarily recover the friction in Eq. (7) [rather than Eq. (11)]. Thus, in the limit of large Γ, Eq. (13) is not exactly equivalent to EF. To correct this feature, one simple approach is to increase BCME friction so that every BCME trajectory experiences an extra damping $\gamma_{e,b}(x) - \gamma_e(x)$. Obviously, this factor is applied if and only if $\gamma_e(x) < \gamma_{e,b}(x)$. Thus, if there is an additional external source of friction γ_{ext}, the final BCME friction becomes

$$\gamma^{BCME}(x) = \gamma_{ext} + \gamma_{e,b}(x) - \gamma_e(x). \tag{14}$$

This concludes our discussion of the BCME.

E. Independent electrons surface hopping (IESH)

Apart from the surface hopping algorithms mentioned above, the most well-established surface hopping protocol for modeling dynamics at a metal surface is Shenvi, Roy, and Tully's IESH model.[15] IESH is a generalization of the fewest switch surface hopping (FSSH)[20] algorithm systems

with many electrons. We will now briefly review the IESH approach.

According to IESH, we begin by rewriting the Hamiltonian in Eq. (2) as

$$\begin{aligned} H &= \frac{p^2}{2m} + U_0(x) + H_{el}, \\ H_{el} &= h(x)d^\dagger d + \sum_{n=1}^{M} \epsilon_n c_n^\dagger c_n + \sum_{n=1}^{M} V_n(x)(d^\dagger c_n + c_n^\dagger d). \end{aligned} \tag{15}$$

If we diagonalize H_{el} in Eq. (15), we obtain a one-electron orbital basis $\{\phi_j\}$ so that we can rewrite the Hamiltonian as[15]

$$H = \frac{p^2}{2m} + U_0(x) + \sum_{j=1}^{N_e} \lambda_j(x) b_j^\dagger b_j \,, \tag{16}$$

where $b_j^\dagger$ and b_j are creation and annihilation operators for ϕ_j, respectively. The electronic eigenstates can then be expressed as Slater determinants $|\mathbf{j}\rangle = |j_1, \ldots, j_{N_e}\rangle$, where $\mathbf{j} \equiv (j_1, \ldots, j_{N_e})$ is a vector of indices denoting occupied orbitals.

Now, the basic *Ansatz* of IESH is to propagate this electronic wave function $|\Psi\rangle$ according to H_{el}, while H_{el} is changing because of nuclear motion. At $t = 0$, $|\Psi\rangle$ is initialized by a specific set of orbitals $|\mathbf{j}\rangle$. Because H_{el} is an electronic Hamiltonian without electron-electron interactions, it follows that the wave function always remains a Slater determinant $|\Psi(t)\rangle = |\psi_1(t)\psi_2(t)\ldots\psi_{N_e}(t)\rangle$.

As for the nuclei, all nuclear motion is propagated along the adiabatic potential energy surface (PES) labeled by $\mathbf{j}$, with energy

$$E(x) = U_0(x) + \sum_{m=1}^{N_e} \lambda_{j_m}(x). \tag{17}$$

To take non-adiabatic affects into account, IESH allows surface hops between different adiabatic, PESs, e.g., from $|\mathbf{j}\rangle$ to $|\mathbf{k}\rangle$, with a probability

$$g_{\mathbf{j}\to\mathbf{k}} = max\left\{\frac{-2Re A_{\mathbf{jk}}^* \dot{x}\xi_{\mathbf{kj}}}{A_{\mathbf{jj}}}\Delta t, 0\right\}. \tag{18}$$

For a hop to occur, the state $|\mathbf{k}\rangle$ can differ from state $|\mathbf{j}\rangle$ by only one orbital at a time, i.e., $|\mathbf{k}\rangle = |k_1 \ldots k_{i-1}k_i k_{i+1} \ldots k_{N_e}\rangle$ and $|\mathbf{j}\rangle = |j_1 \ldots j_{i-1}j_i j_{i+1} \ldots j_{N_e}\rangle = |k_1 \ldots k_{i-1}j_i k_{i+1} \ldots k_{N_e}\rangle$. The derivative coupling in Eq. (18) is defined as $\xi_{\mathbf{kj}} \equiv \langle \phi_{k_i} | \partial_x \phi_{j_i} \rangle$, and $A_{\mathbf{jk}}$ is defined as[15]

$$A_{\mathbf{jk}} = \langle \mathbf{j}|\Psi\rangle\langle\Psi|\mathbf{k}\rangle. \tag{19}$$

For a given $\mathbf{k}$, $\langle \mathbf{k}|\Psi\rangle$ can be evaluated as the determinant of the overlap matrix S (i.e., det(S)), whose elements are

$$S_{pq} = \langle \phi_{k_p} | \psi_q \rangle. \tag{20}$$

Similar to FSSH, IESH imposes a momentum adjustment to enforce energy conservation when a hop takes place, and an upward hop is frustrated if a particle cannot provide sufficient kinetic energy for the adjustment.

Finally, after we have propagated trajectories, if we want to evaluate the impurity population, we use the following expression:

$$N = \sum_{\mu=1}^{N_e} |\langle d|\psi_\mu\rangle|^2. \tag{21}$$

1. IESH with thermostat

One disadvantage of the IESH algorithm described above is that one does not impose a Fermi level for the metal. Instead, the Fermi level characterizing a metal is enforced only by the number of electrons included and effectively one usually assumes zero temperature. Alternatively, one can define a temperature through an ensemble of different IESH initial conditions. In either case, one cannot use IESH to model conduction between two metals with different Fermi levels. Furthermore, without a huge bath of orbitals, the simulation may not be reliable for long times (since there is no external relaxation imposed and detailed balance is not assured). To partly address these issues, Shenvi and Tully have suggested adding an electronic thermostat.[23] With an electronic thermostat, at every time step, with a probability of $\Delta t/\tau$ (where τ is the average time scale of the thermostat), one attempts to hop from an occupied orbital i to an empty orbital a; i and a are picked randomly. If energy $\lambda_a < \lambda_i$, the attempt is accepted immediately; if $\lambda_a > \lambda_i$, then the attempt is accepted with a probability of $e^{-(\lambda_a-\lambda_i)/kT}$.

III. RESULTS

A. Simulation details

The potential surfaces we will investigate are from the standard double-well model[26,28,49]

$$\begin{aligned} U_0(x) &= \frac{1}{2}m\omega^2 x^2, \\ U_1(x) &= \frac{1}{2}m\omega^2(x-g)^2 + \Delta G^o. \end{aligned} \tag{22}$$

The parameters used for our model are (units: a.u.) $m = 2000$, $\omega = 2.0 \times 10^{-4}$, $g = 20.6097$, $\Delta G^o = -3.8 \times 10^{-3}$, and $kT = 9.5 \times 10^{-4}$. The parameters are chosen according to Ref. 28. The corresponding surfaces are plotted in Fig. 1.

For a small Γ, the standard Marcus rate can be evaluated as[28,50]

$$\begin{aligned} k_{Marcus} &= k_{0\to1} + k_{1\to0}, \\ k_{1\to0} &= \int d\epsilon \frac{\Gamma(\epsilon)}{\hbar}(1-f(\epsilon))\frac{e^{-(E_r-\Delta G^o+\epsilon)^2/4E_rkT}}{\sqrt{4\pi E_r kT}}, \\ k_{0\to1} &= \int d\epsilon \frac{\Gamma(\epsilon)}{\hbar}f(\epsilon)\frac{e^{-(E_r+\Delta G^o-\epsilon)^2/4E_rkT}}{\sqrt{4\pi E_r kT}}. \end{aligned} \tag{23}$$

Here the reorganization energy is $E_r \equiv m\omega^2 g^2/2$.

To investigate the dynamics and perform time evolution, we first initialize trajectories at thermal equilibrium in the U_0 well. Unless noted otherwise, the electronic orbitals of

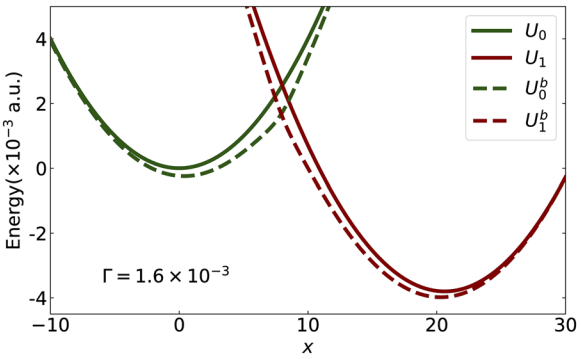

FIG. 1. The original and broadened energy surfaces used in this paper. U_0 and U_1 are the original diabatic surfaces [see Eq. (22)]; U_0^b and U_1^b are the broadened diabatic surfaces with $\Gamma = 1.6 \times 10^{-3}$ [see Eq. (12)].

the metal are prepared at zero temperature (i.e., the lowest orbitals are always occupied). After that, we propagate these trajectories using either BCME, CME, EF, or IESH dynamics. For the propagation, we use the velocity Verlet integrator for the nuclear degree of freedom (DoF) and the RK4 integrator for the electronic DoF. All trajectories are subject to external nuclear friction $\gamma_{ext} = 2m\omega$, which enforces a critical-damping limit rather than an over-damped limit.[72,73] Finally, electron transfer rates are evaluated by fitting the time evolution of the impurity population to the function $Ae^{-kt} + B$. Some of our simulations have been implemented on our own cluster and some have been carried out on the Extreme Science and Engineering Discovery Environment (XSEDE) supercomputer.[51] For IESH, the number of electron N_e is set to be $M/2$ and the lowest N_e orbitals in the band are occupied at $t = 0$. To satisfy the Condon approximation, we let V_n be independent of x. Furthermore, to satisfy the wide band approximation, we choose V_n such that $\Gamma(\epsilon_n) = 2\pi V_n^2 \rho$ is independent of n, i.e.,

$$V_n = \sqrt{\frac{\Gamma}{2\pi\rho}}. \tag{24}$$

Here the density of one electron states is $\rho = M/2W$.

B. Dynamics for different combinations of *W* and *M*

In Fig. 2, we plot the impurity hole population ($1 - N$, where $N = \langle d^\dagger d \rangle$) as a function of time as predicted by both IESH and BCME. Given our intent to explore Marcus theory and the wide band limit, different combinations of bandwidth (2W) and bath orbital number (M) are investigated. We observe that one must be very careful when extrapolating IESH results to the wide band limit: (i) For a given Γ and bandwidth, IESH converges as M increases (but not usually to the wide band limit value). (ii) For a given Γ and density of one electron states $M/2W$, IESH converges as W increases (but again not necessarily to the wide band limit). (iii) For large enough W and large enough $M/2W$, IESH results converge to BCME results and recover the long time equilibrium both for large Γ and small Γ.

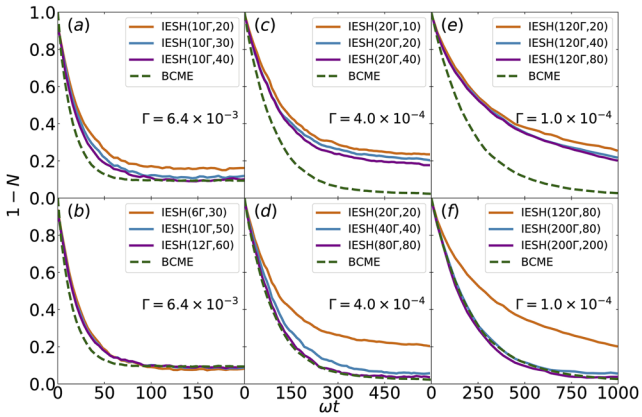

FIG. 2. We plot the hole population of the impurity site ($1 - N(t)$, $N = \langle d^\dagger d \rangle$) for BCME and IESH as a function of time. IESH results are calculated with different combinations of *W* (bandwidth parameter) and *M* (number of bath states). We report results as IESH(2*W*, *M*). See Sec. II A for details. For a given bandwidth, IESH dynamics converge as *M* increases, but these results are not usually in the wide band limit value. If the density of one electron states is large enough, IESH dynamics can be extrapolated to the wide band limit by increasing *W*. Smaller values of Γ require more states (i.e., larger *M*) for convergence. In general, for a large enough bandwidth and large enough density of one electron states, the IESH results closely recover the BCME rates and equilibrium populations, especially for small Γ.

Of course, including a large number of one electron states is computationally demanding and we would prefer a very efficient means to obtain a converged result. As Fig. 2 shows, however, there is no obvious means to obtain such convergence of IESH beyond brute force, i.e., increasing both W and $M/2W$ (see the Appendix for more details). Nevertheless, from these observations, we conclude that the IESH results should reduce to well-known physical results for a wide enough electronic bandwidth and dense enough set of electronic states.

C. Relaxation rates

Next, in Fig. 3, we fit all dynamics to $Ae^{-kt} + B$ and plot relaxation rates as a function of coupling strength (see Table I for exact parameters).[74] For comparison, we also plot results according to Marcus theory,[75] CME, and BCME. The latter results were reported previously in Ref. 28. As discussed in Ref. 28, in the small Γ limit, both the CME and BCME successfully recover the Marcus rate; as Γ increases, Marcus theory predicts too fast a relaxation, while the CME predicts too slow a relaxation. The BCME results can be considered reliable for all different Γ (small or large). From Fig. 3, we observe that IESH rates agree well with BCME rates for small Γ; for large Γ, IESH rates are slightly slower. Although we have not run simulations for even smaller Γ due to the prohibitive computational cost (see Sec. IV A), based on the existing data, it appears that the IESH results should be considered reliable for this model.

As a side note (see Sec. III F), we also notice that including a thermostat degrades the accuracy of IESH dynamics.

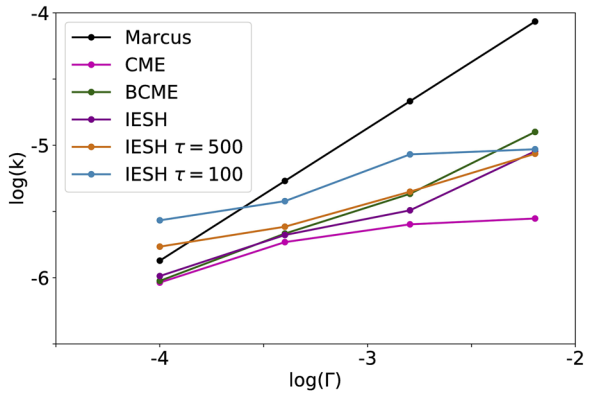

FIG. 3. Relaxation rates as a function of Γ for different algorithms as obtained by fitting $1 - N(t) = Ae^{-kt} + B$. The BCME rates can be considered as very reliable, correctly interpolating from the nonadiabatic regime (where BCME and CME dynamics are identically equal to the Marcus rate) all the way to the adiabatic limit. IESH rates are close to BCME rates for both large and small Γ, suggesting that (when properly converged) IESH should be reliable for this model problem. By adding an electronic thermostat to IESH, the relaxation rates increase when a smaller τ is applied, which would appear to make the results worse (and farther from Marcus theory). Here, to observe a meaningful effect, we have chosen $1/\tau > \Gamma$ for all but one point. Clearly, as the ratio $\Gamma/\tau \to 0$, the IESH dynamics lose accuracy. For discussion of electronic thermostats, see Sec. III F.

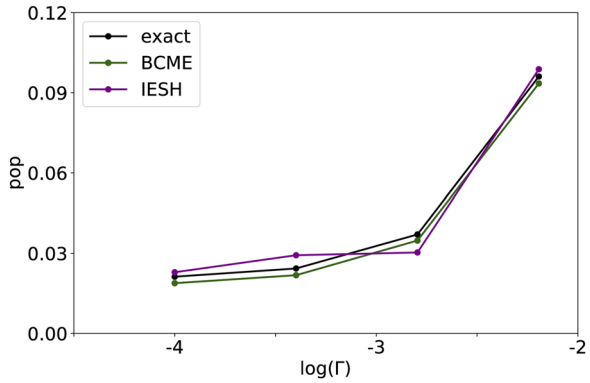

FIG. 4. Equilibrium population as a function of Γ. The exact population is calculated from Eq. (25). Because the BCME reduces to the CME in the small Γ limit (and CME must recover the correct equilibrium population) and the BCME reduces to EF in the large Γ limit (and EF must recover the correct equilibrium population), the BCME algorithm is guaranteed to yield the correct equilibrium population in both the small and large Γ limits. Here we see that IESH also nearly recovers the exact population as well.

D. Long time limit

Beyond dynamics, a useful quantity in the study of nonadiabatic phenomena is the long time equilibrium population. One of the strengths of surface hopping methods is that, because of forbidden hops, these methods should approximately recover the correct equilibrium population[52,53] (and preserve detailed balance). In Fig. 4, we plot equilibrium populations as a function of Γ for both BCME and IESH algorithms. The BCME and IESH equilibrium populations are approximated by the fitting parameter B in $Ae^{-kt} + B$. We also calculate the correct equilibrium population (assuming classical nuclei) using the following formula:[54]

$$N_{eq} = \frac{\int dx n(h(x)) e^{-U_b^{adiab}(x)/kT}}{\int dx e^{-U_b^{adiab}(x)/kT}}. \quad (25)$$

Here $U_b^{adiab}(x)$ is defined in Eq. (8). One can easily verify that both BCME and IESH predict equilibrium populations that are very close to the exact equilibrium population for all Γ.

TABLE I. Parameters and CPU time per trajectory to reach equilibrium. Γ is the hybridization function [Eq. (10)], the band range is $[-W, W]$, M is the number of states, dt is the classical time step, dt_q is the quantum time step, and T is the total time in multiples of dt (i.e., the total number of time steps).

Γ	2W	M	dt	dt_q	T	IESH	BCME (s)
1×10^{-4}	200Γ	200	10	1	5.0×10^5	10 h	0.6
4×10^{-4}	80Γ	80	10	1	3.0×10^5	27 min	0.3
1.6×10^{-3}	10Γ	40	10	1	1.8×10^5	15 min	0.2
6.4×10^{-3}	10Γ	40	10	1	1.2×10^5	10 min	0.2

E. External friction

At this point, we have shown that, when converged with regards to W and M, the IESH results mimic the BCME results almost quantitatively. And yet this equivalence must be surprising. After all, without an electronic thermostat, IESH dynamics are partly ignorant of temperature. The initial electronic state is at 0 K. All temperature information is stored only through (i) the initial distribution of velocity for the nuclear trajectories and (ii) the external nuclear friction.

With this in mind, we now explore the influence of external friction on all dynamics. Whereas all previous results were obtained with external nuclear friction $\gamma_{ext} = 2m\omega$, we will now set $\gamma_{ext} = 0$ and evolve the system without any external friction. The trajectories are prepared with the nuclear position and velocity equilibrated to a temperature $kT_0 = 5kT$. For these simulations, we will initially populate all metallic orbitals according to a Boltzmann distribution at a finite temperature (as given by an electronic thermostat). In other words, we turn a thermostat *on* during equilibration (when nuclei are frozen), but we turn the thermostat *off* during the actual nuclear dynamics period (when the nucleus is allowed to move). All the results are plotted in Fig. 5. For reference, we plot the results using CME, BCME, and broadened EF.

From the short time data in Fig. 5, we find that, without external nuclear friction, BCME always predicts a much faster electronic relaxation than IESH (for both BCME flavors). In fact, IESH dynamics appear to relax even more slowly than both CME and EF dynamics, which suggests that these dynamics may not be accurate; after all, since CME and EF represent opposite extremes, one might expect the correct relaxation

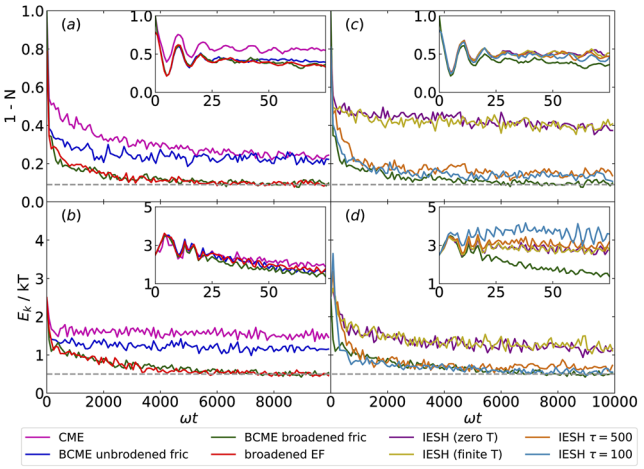

FIG. 5. Time evolution for the zero external nuclear friction case. We plot both the population of the hole impurity ($1 - N$) as well as the nuclear kinetic energy (E_k). Here $\Gamma = 6.4 \times 10^{-3}$, $\gamma_{ext} = 0$. For clarity, eight algorithms are plotted separately: (a) the electronic relaxation according to CME, the two flavors of BCMEs (without broadened friction and with broadened friction), and broadened EF; (b) the kinetic energy relaxation according to CME, BCME, and broadened EF; (c) the electronic relaxation according to BCME with broadened friction, IESH (zero T), IESH (finite T), and IESH with the electronic thermostat; (d) the kinetic energy relaxation according to BCME with broadened friction, IESH (zero T), IESH (finite T), and IESH with the electronic thermostat. The small window on each plot represents the corresponding short time dynamics. The system is initially prepared at $5kT$ so that $E_k = 2.5kT$ at time zero. Only 250 trajectories are used here due to the prohibitive computational cost of IESH. Gray dashed lines are the correct equilibrium limits. For electronic population, IESH relaxes much slower than either BCME or electronic friction. In fact, IESH relaxes even more slowly than the CME, indicating that the IESH electronic dynamics may not be believable. For nuclear dynamics, BCME with either broadened friction or broadened electronic friction relaxes to the correct kinetic energy limit (while IESH does not). Furthermore, IESH dynamics do not appear to be sensitive to the initial electron temperature (zero T *vs* finite T). By adding an electronic thermostat, IESH can recover both the correct electronic population and nuclear kinetic energy at long times. Here, we choose two different relaxation times $\tau = 100$ and $\tau = 500$ so that we have $1/\tau > \Gamma$ and $1/\tau < \Gamma$. In both cases, however, the short time dynamics are unchanged and slow compared to all other approaches.

rate to lie somewhere between these limits. Perhaps most interestingly, for nuclear dynamics, we find that both BCME (with broadened friction)[76] and electronic friction recover the correct population and kinetic energy, while IESH does not (at least for all times we can afford computationally).

To explain these features, we note that, when modeling this closed system with zero nuclear friction case, IESH trajectories appear to oscillate back and forth without enough energy dissipation such that the system apparently does not reach equilibrium correctly in a measured time. Furthermore, the dynamics of the impurity population (as predicted by IESH) appear not to depend on initial conditions [see "IESH (finite T)" and "IESH (zero T)" in Fig. 5]. Altogether, from Fig. 5, one can hypothesize that IESH does not necessarily recover the correct long time equilibrium state.[77] That being said, according to the data in Figs. 2 and 3, the presence of external nuclear friction correctly fixes up this IESH problem; including

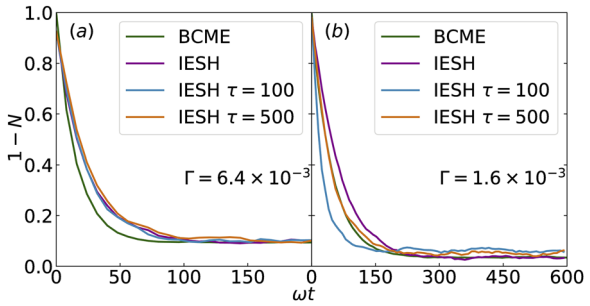

FIG. 6. Time evolution for IESH with an electronic thermostat in the presence of external friction. (a) $\Gamma = 6.4 \times 10^{-3}$. We note that different τ do not yield significant differences; (b) $\Gamma = 1.6 \times 10^{-3}$. Not surprisingly, we find that including an electronic thermostat increases the relaxation rate: The smaller the τ, the faster the relaxation. In this case, we also see a slightly increased value of $1 - N$ at equilibrium in the presence of an electronic thermostat.[78]

external friction and random force for the nuclei can compel the electronic system to equilibrate correctly to a nonzero temperature (rather than the metallic electronic system forcing the nuclei to freeze and approach 0 K).

F. IESH with electronic thermostat

From the data in Figs. 3 and 5, we see that IESH can match Marcus theory and BCME in the presence of external friction so as to drive equilibration at long times; without external friction, equilibrium may not be reached. As emphasized above, however, another approach for driving IESH to equilibrium is to add an electronic thermostat. Thus, in Fig. 6, we show that adding such a thermostat can indeed speed up the relaxation rates in the presence of external friction while slightly increasing the equilibrium population.[78] It is observed that, for the $\Gamma = 6.4 \times 10^{-3}$ case (see the left panel in Fig. 6), the dynamics with different τ are basically identical; while for $\Gamma = 1.6 \times 10^{-3}$ case (right panel in Fig. 6), the relaxation is significantly faster for smaller τ. The effects of thermostats on relaxation rates are also plotted in Fig. 3. From the data, one can surmise a simple trend here: using an IESH thermostat results in a faster relaxation rate. We note that sometimes this faster rate is more accurate than dynamics without a thermostat; other times, including a thermostat leads to worse results[79] (Figs. 3 and 6).

Finally we can also investigate the effect of a thermostat for the zero external friction case. Results for IESH with different τ are plotted in Fig. 5. We find that the IESH results with a thermostat do reach the correct long time limit much faster than running dynamics without a thermostat, both for electronic population and nuclear kinetic energy. However, for short time dynamics, adding a thermostat turns out to have almost no affect.

IV. DISCUSSION

Thus far we have shown that IESH is a reliable algorithm in the presence of external friction and that IESH recovers

Marcus theory when the bandwidth is large enough. However, the accuracy of IESH would appear to be dependent on the presence of external friction to drive the dynamics to the correct equilibrium. At this point, there are a few details we would like to discuss.

A. Simulation cost

A summary of the computational time required for the system to reach equilibrium is listed in Table I. In practice, we notice that, in order to recover converged results, the computational cost of IESH is typically much more expensive than that of BCME (>1000 times). The computational cost of IESH depends strongly on the bath discretization scheme, as the algorithm treats bath orbitals explicitly; the algorithm scales $\sim M^2$, where M is the number of the bath orbitals. Clearly, there is a strong need to use improved sampling for the manifold of bath states. Unfortunately so far, we have not been able to recover converged results easily with the discretization scheme proposed in Ref. 15 (see the Appendix for details). Without an effective discretization scheme, the BCME algorithm is obviously a much cheaper (though less general) algorithm for simulating metal-molecule electron transfer for large systems.

B. Obstacles for progress

Although both the BCME and IESH performed reasonably well in the 1-D model in Eq. (22), there are still many questions to be answered. First, with regard to BCME, in order to simulate a realistic system, we must go beyond the wide band approximation. Doing so will require a nontrivial extension of BCME dynamics, which presumably can be accomplished through the addition of multiple molecular orbital levels.[55] This remains to be accomplished. Second, with regard to IESH, another open question is, how to choose an optimized relaxation time τ? And, in particular, without external friction, is there a robust approach for choosing τ whereby we recover the correct equilibrium results without sacrificing accurate short time dynamics? Finally, we can always wonder: is it possible to somehow combine BCME and IESH so that we can obtain a scheme that is both cheap and generalizable? We do not yet have answers for these questions, and this is an exciting time to study dynamics near a metal surface.

V. CONCLUSIONS AND OUTLOOK

To summarize, we have investigated molecule-metal electron transfer within a generalized AH model with two different surface hopping algorithms: BCME and IESH. We find that:

- IESH can produce converged dynamics only if both the bandwidth (2W) and the number of the one electron states are large enough.
- In the presence of external friction, the converged IESH results typically agree with the BCME results for both relaxation rates and equilibrium populations. In the small Γ limit, both sets of results recover the Marcus rate. As Γ increases, the IESH relaxation rates are slightly smaller than the BCME results. IESH always recovers an accurate equilibrium population at long time.
- In the limit of zero nuclear friction, IESH predicts an extremely slow electronic relaxation rate and is not able to recover the equilibrium kinetic energy or electronic populations within a computationally feasible amount of time. Apparently, IESH is not able to predict the correct dynamics without the presence of external friction to maintain the correct temperature for long times.
- Adding an electronic thermostat to IESH apparently increases all relaxation rates. As τ gets smaller, these relaxation rates always increase. For the case of zero nuclear friction limit, including an IESH thermostat successfully recovers the correct electronic population and kinetic energy for the system at equilibrium, but the accuracy of short time dynamics is unknown.

Overall, given that surface hopping methods are very often the only feasible dynamics algorithms for modeling coupled nuclear-electronic dynamics near a metal surface where nuclear motion can be considered classical, let us now summarize the status of surface hopping dynamics, IESH *vs* BCME, for those wishing to run practical simulations. On the one hand, BCME dynamics have been benchmarked against exact quantum dynamics[29] for steady-state currents and we believe these dynamics should be accurate for modeling metal-molecule electron transfer in the limit of high temperatures (such that all nuclear motion can be considered classical). These dynamics are guaranteed to reach the correct thermal equilibrium; they are also very computationally efficient. The downside of these dynamics is that it is difficult to include more than two electron states of the same charge; including multiple states necessitates merging BCME dynamics with standard FSSH dynamics, which has not yet been fully optimized (despite encouraging initial results[55]).

On the other hand, IESH dynamics are far more general than BCME dynamics and can treat arbitrarily many excited states (provided there are no electron-electron interactions). That being said, however, IESH is far more expensive than BCME, and the present results indicate that IESH will not necessarily be reliable for gas phase molecule-metal scattering. Nevertheless, for reactions at a metal-liquid interface, all indications are that IESH dynamics should be as reliable as FSSH calculations in solution (again provided electron-electron interactions are not crucial). Future development of the IESH approach may well benefit from comparisons against a rigorous quantum-classical Liouville equation,[36,41–45] along the lines of what has been achieved for FSSH with a handful of electronic states.[43,56] Just as decoherence corrections improved the FSSH algorithm,[57–68] minor changes to the IESH algorithm may well lead to improved accuracy.

Finally, before concluding, we should emphasize that our outlook above must be regarded with just a small grain of salt. Without exact quantum data, we have used Marcus theory and basic common sense to assess the performance of IESH vis-a-vis BCME dynamics. In the future, the field of metal-molecule dynamics will greatly benefit from the presence of easily available benchmark data for the non-equilibrium dynamics of a particle near a metal. Such data should be possible, in principle, using either the hierarchical quantum master equation (HQME)[69] or the real time quantum Monte Carlo approaches.[70,71] We hope this paper helps spur the creation of such a necessary benchmarking data set.

ACKNOWLEDGMENTS

This material is based upon work supported by the (U.S.) Air Force Office of Scientific Research (USAFOSR) award under AFOSR Grant No. FA9550-18-1-0497. This work used the Extreme Science and Engineering Discovery Environment (XSEDE), which is supported by National Science Foundation Grant No. ACI-1548562. J.S. acknowledges the David and Lucille Packard Fellowship. We also acknowledge Huike Jin for very helpful discussions regarding code optimization and Sascha Kandratsenka and Dan Auerbach for very useful insight into the IESH algorithm.

APPENDIX: PRACTICAL CONVERGENCE OF IESH TO THE WIDE BAND LIMIT

1. Convergence criteria

The results in Fig. 2 indicate that IESH will converge to the BCME results in the limits of large W and large M. To understand why convergence appears tricky, note the following three conditions:

1. To reach the wide band limit, the metal bandwidth 2W must be significantly larger than the coupling strength Γ (i.e., $2W \gg \Gamma$).
2. Consider the schematic diabatic states plotted in Fig. 7. When a particle is moving along an adiabatic corresponding to a single electron determinant electron states, the particle can hop only to those states that differ by a single orbital; states differing by more than one orbital are only indirectly coupled. Thus, for example, in Fig. 7, let 1 be the initial state. Note that 1 is directly coupled to 1′, 2′, and 4′, but not to 3′; 2′ is directly coupled to 1 and 3, but not to 2, etc.

   As the simulation moves forward, a particle effectively hops back and forth between states with the impurity occupied or unoccupied, and the bandwidth must be chosen to be large enough such that trajectories can sample all such relevant states (1, 1′, 2, 2′, 3, 3′, 4′,. . .). For particles initialized with the impurity unoccupied at temperature kT, given that a reactive trajectory needs only to cross the barrier from a donor to an acceptor, the highest possible energy they must sample is roughly $E_{barrier}$ + O(1)∗kT. Here, for a converged result, we may safely assume that barrier crossings occur with no more than $3kT$ of excess energy.

   Finally, for the model problem in Fig. 2, the donor and acceptor energy surfaces are not symmetric. Thus in order to reach the thermal equilibrium, all states below E_{bath} + $3kT$ must be equivalently sampled. For our purposes, this implies that for converged results, we must choose the benchmark of metallic one-electron orbitals to be $W \approx |\Delta G^o| + E_{barrier} + 3kT \approx 0.032$. According to Fig. 2, such a choice does yield approximately converged results.
3. As we are interested in an irreversible electron transfer process between a molecule and a bath, the energy spacing between the neighboring states must be small compared to the molecule-metal coupling. In other words, we require a large enough density of states. Note that this requirement is not as strong as enforcing $2W/M \ll \Gamma$ as the spacing between many body states need not necessarily be equal to the spacing between one electron states in the bath. Obviously, the former may be much smaller than the latter. That being said, in the small Γ limit, we find that the number of bath orbitals M must be quite large to satisfy all of the requirements above.

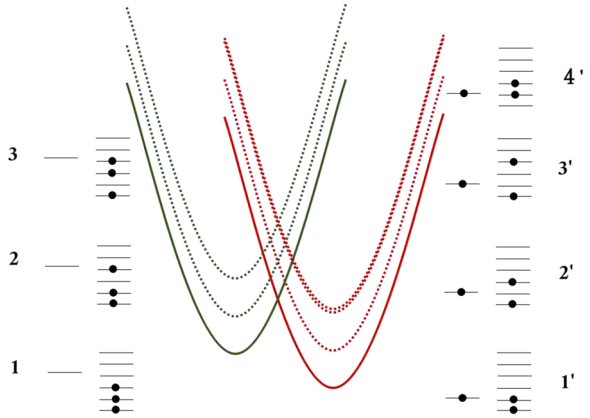

FIG. 7. Schematic diabatic states of the system. The solid lines and dashed lines are the ground and excited diabatic states, respectively. The red lines represent states with the impurity orbital occupied, while the green lines represent states with the impurity orbital unoccupied. Several representative electron distributions for unoccupied and occupied states are also plotted. Note that states 3′ and 4′ are degenerate. The hopping map of possible hopping schemes is complicated. The initial state 1 is coupled to states 1′, 2′, and 4′; state 1′ is coupled to states 1 and 2; and state 2 is coupled to states 1′ and 3′. The requirements for reaching equilibrium are very demanding in the small Γ limit.

Altogether, these requirements explain why the IESH simulation is hard to converge as Γ decreases in Fig. 2.

2. Non-uniform discretization schemes

As we stated in Sec. IV, an optimal discretization scheme should predict the correct dynamics while keeping the number of bath orbitals relatively small. However to capture accurate dynamics with a non-uniform discretization scheme,

one must at the very least be sure that the set of bath orbitals near the Fermi level form a dense manifold. That being said, at the same time, to save computational cost, the one-electron orbitals far from the Fermi level must be more sparsely distributed—while still finding the correct long time equilibrium limit as well.

In our calculations, we have found it is extremely hard to find such a numerically well-defined density of one electron states that can produce the correct, converged results when there are only 20-80 orbitals in total. For small Γ, we always find that a very broad set of bath orbitals is necessary for the reasons discussed above. To make problems worse, we also find that defining the density of one electron states ρ as the difference between energy levels can be numerically unstable for certain discretizations, yet such a density of one electron states is necessary to form the correct overall decay rate $\frac{\Gamma}{\hbar} = \frac{2\pi\rho}{\hbar}V^2$. For this reason, we have stuck here with a safe, but expensive, uniform discretization, rather than Shenvi's discretization scheme.[15]

REFERENCES

[1] Y. Huang, C. T. Rettner, D. J. Auerbach, and A. M. Wodtke, Science **290**, 111 (2000).
[2] J. D. White, J. Chen, D. Matsiev, D. J. Auerbach, and A. M. Wodtke, Nature **433**, 503 (2005).
[3] V. Krishna and J. C. Tully, J. Chem. Phys. **125**, 054706 (2006).
[4] C. Bartels, R. Cooper, D. J. Auerbach, and A. M. Wodtke, Chem. Sci. **2**, 1647 (2011).
[5] A. M. Wodtke, Chem. Soc. Rev. **45**, 3641 (2016).
[6] A. Nitzan, Annu. Rev. Phys. Chem. **52**, 681 (2001).
[7] A. Kandratsenka, H. Jiang, Y. Dorenkamp, S. M. Janke, M. Kammler, A. M. Wodtke, and O. Bünermann, Proc. Natl. Acad. Sci. U. S. A. **115**, 680 (2018).
[8] J. C. Tully, *Theoretical Chemistry Accounts* (Springer, 2000), pp. 173–176.
[9] A. M. Wodtke, J. C. Tully, and D. J. Auerbach, Int. Rev. Phys. Chem. **23**, 513 (2004).
[10] B. C. Krüger, N. Bartels, C. Bartels, A. Kandratsenka, J. C. Tully, A. M. Wodtke, and T. Schäfer, J. Phys. Chem. C **119**, 3268 (2015).
[11] G. Stock and M. Thoss, Phys. Rev. Lett. **78**, 578 (1997).
[12] S. M. Janke, D. J. Auerbach, A. M. Wodtke, and A. Kandratsenka, J. Chem. Phys. **143**, 124708 (2015).
[13] M. Head-Gordon and J. C. Tully, J. Chem. Phys. **103**, 10137 (1995).
[14] M. Brandbyge, P. Hedegård, T. Heinz, J. Misewich, and D. Newns, Phys. Rev. B **52**, 6042 (1995).
[15] N. Shenvi, S. Roy, and J. C. Tully, J. Chem. Phys. **130**, 174107 (2009).
[16] W. Dou and J. E. Subotnik, J. Chem. Phys. **144**, 024116 (2016).
[17] S. Monturet and P. Saalfrank, Phys. Rev. B **82**, 075404 (2010).
[18] S. P. Rittmeyer, J. Meyer, J. I. Juaristi, and K. Reuter, Phys. Rev. Lett. **115**, 046102 (2015).
[19] S. Li and H. Guo, J. Chem. Phys. **117**, 4499 (2002).
[20] J. C. Tully, J. Chem. Phys. **93**, 1061 (1990).
[21] N. Shenvi, S. Roy, and J. C. Tully, Science **326**, 829 (2009).
[22] R. Cooper, C. Bartels, A. Kandratsenka, I. Rahinov, N. Shenvi, K. Golibrzuch, Z. Li, D. J. Auerbach, J. C. Tully, and A. M. Wodtke, Angew. Chem. **124**, 5038 (2012).
[23] N. Shenvi and J. C. Tully, Faraday Discuss. **157**, 325 (2012).
[24] A. M. Wodtke, Y. Huang, and D. J. Auerbach, J. Chem. Phys. **118**, 8033 (2003).
[25] N. Bartels, B. C. Krüger, D. J. Auerbach, A. M. Wodtke, and T. Schäfer, Angew. Chem., Int. Ed. **53**, 13690 (2014).
[26] W. Dou, A. Nitzan, and J. E. Subotnik, J. Chem. Phys. **143**, 054103 (2015).
[27] W. Dou and J. E. Subotnik, J. Chem. Phys. **146**, 092304 (2017).
[28] W. Ouyang, W. Dou, A. Jain, and J. E. Subotnik, J. Chem. Theory Comput. **12**, 4178 (2016).
[29] W. Dou, C. Schinabeck, M. Thoss, and J. E. Subotnik, J. Chem. Phys. **148**, 102317 (2018).
[30] G. Miao, W. Dou, and J. Subotnik, J. Chem. Phys. **147**, 224105 (2017).
[31] M. Galperin, M. A. Ratner, and A. Nitzan, Nano Lett. **5**, 125 (2005).
[32] M. Galperin, M. A. Ratner, and A. Nitzan, J. Phys.: Condens. Matter **19**, 103201 (2007).
[33] M. Delbecq, V. Schmitt, F. Parmentier, N. Roch, J. Viennot, G. Fève, B. Huard, C. Mora, A. Cottet, and T. Kontos, Phys. Rev. Lett. **107**, 256804 (2011).
[34] F. Cavaliere, E. Mariani, R. Leturcq, C. Stampfer, and M. Sassetti, Phys. Rev. B **81**, 201303 (2010).
[35] W. Dou and J. E. Subotnik, Phys. Rev. B **96**, 104305 (2017).
[36] W. Dou and J. E. Subotnik, Phys. Rev. B **97**, 064303 (2018).
[37] N. Bode, S. V. Kusminskiy, R. Egger, and F. von Oppen, Beilstein J. Nanotechnol. **3**, 144 (2012).
[38] J. Daligault and D. Mozyrsky, Phys. Rev. E **75**, 026402 (2007).
[39] B. B. Smith and J. T. Hynes, J. Chem. Phys. **99**, 6517 (1993).
[40] M. S. Mizielinski, D. M. Bird, M. Persson, and S. Holloway, J. Chem. Phys. **122**, 084710 (2005).
[41] R. Kapral and G. Ciccotti, J. Chem. Phys. **110**, 8919 (1999).
[42] S. Nielsen, R. Kapral, and G. Ciccotti, J. Chem. Phys. **112**, 6543 (2000).
[43] R. Kapral, Chem. Phys. **481**, 77 (2016).
[44] C. C. Martens and J.-Y. Fang, J. Chem. Phys. **106**, 4918 (1997).
[45] A. Donoso and C. C. Martens, J. Phys. Chem. A **102**, 4291 (1998).
[46] W. Dou and J. E. Subotnik, J. Chem. Phys. **145**, 054102 (2016).
[47] W. Dou, G. Miao, and J. E. Subotnik, Phys. Rev. Lett. **119**, 046001 (2017).
[48] M. Esposito, M. A. Ochoa, and M. Galperin, Phys. Rev. Lett. **114**, 080602 (2015).
[49] A. Nitzan, *Chemical Dynamics in Condensed Phases: Relaxation, Transfer and Reactions in Condensed Molecular Systems* (Oxford University Press, 2006).
[50] W. Dou, A. Nitzan, and J. E. Subotnik, J. Chem. Phys. **142**, 234106 (2015).
[51] J. Towns, T. Cockerill, M. Dahan, I. Foster, K. Gaither, A. Grimshaw, V. Hazlewood, S. Lathrop, D. Lifka, G. D. Peterson *et al.*, Comput. Sci. Eng. **16**, 62 (2014).
[52] P. V. Parandekar and J. C. Tully, J. Chem. Phys. **122**, 094102 (2005).
[53] J. Schmidt, P. V. Parandekar, and J. C. Tully, J. Chem. Phys. **129**, 044104 (2008).
[54] W. Dou, A. Nitzan, and J. E. Subotnik, J. Chem. Phys. **144**, 074109 (2016).
[55] W. Dou and J. E. Subotnik, J. Chem. Theory Comput. **13**, 2430 (2017).
[56] B. R. Landry, M. J. Falk, and J. E. Subotnik, "Communication: The correct interpretation of surface hopping trajectories: How to calculate electronic properties," J. Chem. Phys. **139**, 211101 (2013); J. E. Subotnik, W. Ouyang, and B. R. Landry, "Can we derive Tully's surface-hopping algorithm from the semiclassical quantum Liouville equation? Almost, but only with decoherence," *ibid.* **139**, 214107 (2013).
[57] B. J. Schwartz, E. R. Bittner, O. V. Prezhdo, and P. J. Rossky, J. Chem. Phys. **104**, 5942 (1996).
[58] A. Jain, E. Alguire, and J. E. Subotnik, J. Chem. Theory Comput. **12**, 5256 (2016).
[59] E. R. Bittner and P. J. Rossky, J. Chem. Phys. **103**, 8130 (1995).
[60] J. E. Subotnik and N. Shenvi, J. Chem. Phys. **134**, 244114 (2011).
[61] J. E. Subotnik and N. Shenvi, J. Chem. Phys. **134**, 024105 (2011).
[62] H. M. Jaeger, S. Fischer, and O. V. Prezhdo, J. Chem. Phys. **137**, 22A545 (2012).
[63] B. R. Landry and J. E. Subotnik, J. Chem. Phys. **137**, 22A513 (2012).

[64]J.-Y. Fang and S. Hammes-Schiffer, J. Phys. Chem. A **103**, 9399 (1999).
[65]J.-Y. Fang and S. Hammes-Schiffer, J. Chem. Phys. **110**, 11166 (1999).
[66]M. D. Hack and D. G. Truhlar, J. Chem. Phys. **114**, 2894 (2001).
[67]Y. L. Volobuev, M. D. Hack, M. S. Topaler, and D. G. Truhlar, J. Chem. Phys. **112**, 9716 (2000).
[68]A. W. Jasper and D. G. Truhlar, J. Chem. Phys. **123**, 064103 (2005).
[69]C. Schinabeck, A. Erpenbeck, R. Härtle, and M. Thoss, Phys. Rev. B **94**, 201407 (2016).
[70]L. Mühlbacher and E. Rabani, Phys. Rev. Lett. **100**, 176403 (2008).
[71]G. Cohen, E. Gull, D. R. Reichman, A. J. Millis, and E. Rabani, Phys. Rev. B **87**, 195108 (2013).
[72]L. Zusman, Chem. Phys. **49**, 295 (1980).
[73]A real metal consists of many atoms that are non-static. To approximate the phononic couplings between a metal and a molecule, external nuclear friction on the molecule can be applied. Here, in order to use this Marcus rate as a reference, we choose the critical damping limit $\gamma_{ext} = 2m\omega$. Otherwise, for example, if we were to choose over-damped nuclear friction, we would need to benchmark against Zusman's rate.
[74]Because of the large computational cost, for the $\Gamma = 1.0 \times 10^{-4}$ case, we set $W = 200\Gamma$ and $M = 200$ for standard IESH dynamics. Furthermore, for this same Γ, when we apply an electronic thermostat, we set $W = 200\Gamma$ and $M = 80$. Figure 3(f) suggests that the difference between these two sets of parameters should be very small and thus we expect this replacement should be reasonable. For CME and BCME, we use 10 000 trajectories; for IESH, we use 1000 trajectories.
[75]For the Marcus theory results, we plot rates $k = k_{0\to1} + k_{1\to0}$; see Eq. (23).
[76]As a side note, one can notice from Fig. 5 that BCME without broadening friction does not agree with EF here, indicating that a broadening of friction can sometimes be crucial. This conclusion was not found in any previous work,[16,27,29] where the influence of broadening friction was always negligible (at least compared to broadening of the potential energy surface).
[77]This hypothesis can only be made tentatively. For instance, in Fig. 5, one might also predict that BCME with unbroadened friction does not reach the correct equilibrium. This prediction would be incorrect, however. BCME dynamics will always reach the correct equilibrium (no matter the friction). And yet, one must be concerned by the fact that IESH dynamics seemingly do not depend on the initial temperature of the metal. Hence, we now tentatively hypothesize that IESH will not reach the correct equilibrium state, even at very, very long times.
[78]We presume that the slight increase in electronic population in Fig. 5(d) induced by the electronic thermostat is caused by our incompatible use of relaxation operators: (i) A Monte Carlo scheme for electronic DoF of the metal combined with (ii) IESH dynamics for the nucleus. Our presumption is that this treatment can lead to a slightly increased effective temperature.
[79]This observation indicates that, for a thermostat to be useful, $1/\tau$ should actually be set as a function of Γ, which is somewhat problematic since τ should be a property of the bath alone. In practice, for a meaningful correction, one would expect that, at a minimum, the bath should equilibrate faster than the molecule-metal energy transfer, i.e., $1/\tau > \Gamma$; we have chosen to investigate τ with this constraint in mind. Finally, given the practical need for a Γ-dependent choice of $1/\tau$, in Fig. 6, we have also investigated thermostats with both $1/\tau > \Gamma$ and $1/\tau < \Gamma$. In both cases, we predict the correct long time equilibrium population, but the dynamics never agree with BCME for short time dynamics. Therefore, our tentative conclusion is that, even with a Γ-dependent choice of $1/\tau$, we do not seem able to find a good compromise between short and long time dynamics.